


Inherent flame-retardant vinyl ester resins with improved heat resistance enabled by additional P/N-containing cross-linking points

Mei Qiu¹ | Xi Chen^{2,3} | Jun Wang^{1,3} | Jingsheng Wang¹ | Kaiwen Chen¹ | Shuang Yang^{2,3}  | Siqi Huo⁴ | Hao Wang⁴

¹School of Materials Science and Engineering, Wuhan University of Technology, Wuhan, China

²School of Mechanical and Electronic Engineering, Wuhan University of Technology, Wuhan, China

³Institute of Advanced Material Manufacturing Equipment and Technology, Wuhan University of Technology, Wuhan, China

⁴Center for Future Materials, University of Southern Queensland, Springfield, Queensland, Australia

Correspondence

Shuang Yang, School of Mechanical and Electronic Engineering, Wuhan University of Technology, Wuhan, China. Email: ysfrp@whut.edu.cn

Siqi Huo, Center for Future Materials, University of Southern Queensland, Springfield, Queensland, Australia. Email: sqhuo@hotmail.com

Funding information

Australia Research Council Discovery Early Career Researcher Award, Grant/Award Number: DE230100616; Science and Technology Department of Jiangsu Province in China, Grant/Award Number: BA2019043

Abstract

Due to the plasticizing effect, the phosphorus-derived flame retardants often imparted flame retardancy to thermosetting resins at the expense of heat resistance. To address this issue, the phosphorous/nitrogen flame retardant (DOPO-TGIC) and 4,4'-diphenyl methane diisocyanate (MDI) were covalently introduced into the cross-linked network of vinyl ester resin (VER) by the reaction of the —OH groups in DOPO-TGIC and VER and the —NCO groups in MDI. Thus, an intrinsically flame-retardant VER was obtained. The as-prepared VER sample exhibited increased glass-transition temperature (T_g) relative to virgin VER sample because DOPO-TGIC served as an additional cross-linking point during curing. Meanwhile, the P/N-containing VER sample featured superior flame-retardant properties, with a UL-94V-0 classification. Compared with VER sample, the peak heat release rate (PHRR) and total heat release (THR) of the P/N-containing VER sample were reduced by 55.6% and 44.0%, respectively. The improved flame retardancy was mainly due to the suppressed burning reaction in the gas phase and improved carbonization capacity in the condensed phase. Therefore, this work proposes a novel and effective strategy for addressing the trade-off between T_g and flame retardancy of thermosetting resins.

KEYWORDS

flame retardancy, heat resistance, P/N-containing flame retardant, vinyl ester resin

1 | INTRODUCTION

In recent years, vinyl ester resin (VER) has been widely applied in coatings, wind turbine blades, electrochemical devices, construction and so on, because of great mechanical properties, processability and corrosion resistance.^{1,2} Unfortunately, the common VER suffers from poor flame retardancy, which greatly limits

its application in the fields with flame retardancy requirements.^{3–5} Therefore, the flame retardant modification of VER is of great significance.

Among many commercial flame-retardants, halogen-containing flame-retardants have the characteristics of large market scale and wide application range, but their burning processes are often accompanied with the release of corrosive or toxic gases, such as dibenzo-p-dioxin and

dibenzofuran, which are very harmful to human beings and ecological environment.^{6–8} As environmental protection and flame retardant regulations become increasingly strict, there is an urgent need for the development of environmentally-friendly flame retardants and fire-retardant materials.^{9–12} Therefore, the non-halogen alternatives, for example, phosphorus (P)-, nitrogen (N)-, and silicon (Si)-containing compounds, have been developed rapidly.^{13–16}

Many non-halogen flame-retardants, especially those containing phosphorus, have been applied in VER, and show obvious flame retardancy.^{17–20} For instance, Ji et al. reported a P/N-containing flame-retardant (PHT), which was applied to improve the flame retardancy and smoke suppression of VER.¹⁸ Their result presented that adding 15 wt% of PHT increased the LOI to 29.0%, and reduced the peak heat release rate and total smoke production by 39.3% and 31.9%, respectively, compared with those of VER. However, the PHT-containing VER sample cannot achieve any UL-94 rating, and its T_g was decreased with the increasing PHT amount. Similarly, Zhang et al. synthesized a P-containing 1-vinylimidazole salt (VIDOP) for the fabrication of flame-retardant VER and its glass fiber reinforced composite.²¹ As expected, VIDOP significantly enhanced the flame retardancy of VER and its glass fiber reinforced composite, but also reduced the T_g . Obviously, the majority of P-containing flame retardants endowed VER with flame retardancy at the expense of glass-transition temperature due to the plasticizing effect, thereby limiting their practical applications. Hence, it is critical yet challenging to address the trade-off between flame retardancy and glass-transition temperature of P-containing VER.

In this work, the phosphaphenanthrene/triazine-trione-containing DOPO-TGIC and MDI were used as additional cross-linking point and bridging agent, respectively, in the VER system. Both DOPO-TGIC and MDI were covalently connected with the cross-linked network of VER by the reaction between $-\text{OH}$ in DOPO-TGIC and VER and $-\text{NCO}$ in MDI. Thus, the intrinsic flame-retardant VER systems were obtained. The thermal properties as well as flame retardancy of the P/N-containing VER were characterized and compared with those of the unmodified VER. Due to the covalent linkage, the as-prepared flame-retardant VER systems exhibited increased T_g values relative to that of pure VER. Finally, the flame-retardant mode-of-action of the P/N-containing VER systems was studied in detail.

2 | EXPERIMENTAL

2.1 | Materials

VER was purchased from Yixing Xinghe Resin Co. LTD. 1,3,5-triglycidyl isocyanurate (TGIC) was purchased

from Wuhan Yuqing Jiaheng Pharmaceutical Co., LTD. 9, 10-dihydro-9-oxa-10-phosphoheterofi-10-oxide (DOPO) was provided by Shanghai Jiuju Chemical Technology Co., LTD. 4,4'-diphenylmethane diisocyanate (MDI), styrene (St) and dibenzoyl peroxide (BPO) were obtained from Aladdin Industries Co., Ltd. Ditin butyl dilaurate was bought from Guangdong Yunxing Biotechnology Co., LTD. The phosphaphenanthrene/triazine-trione-containing flame retardant (DOPO-TGIC, see Scheme 1) was synthesized based on a previous work.²²

2.2 | Preparation of flame-retardant VERs

MDI (7.5 g, 0.03 mol), ditin butyl dilaurate and St were added into a three-neck flask, and stirred intensely to form a transparent solution. Then, DOPO-TGIC (5.1 g, 0.01 mol) was added in batches to the flask, and then the mixture was heated to 180°C and stirred continuously to dissolve DOPO-TGIC. VER was added to the above solution and stirred for 30 min. After the solution was cooled to 65°C, 2 wt% BPO as an initiator was added and stirred for 5 min. The mixture was degassed under vacuum for 5 min, it was poured into a preheated mold and cured at 80, 100, and 140°C for 2 h each. The formation of cross-linked structures for VER samples is shown in Scheme 2. Furthermore, the virgin VER was also prepared in the similar procedure but without the addition of DOPO-TGIC, MDI and dibutyltin dilaurate. The formulations of VER samples are listed in Table 1.

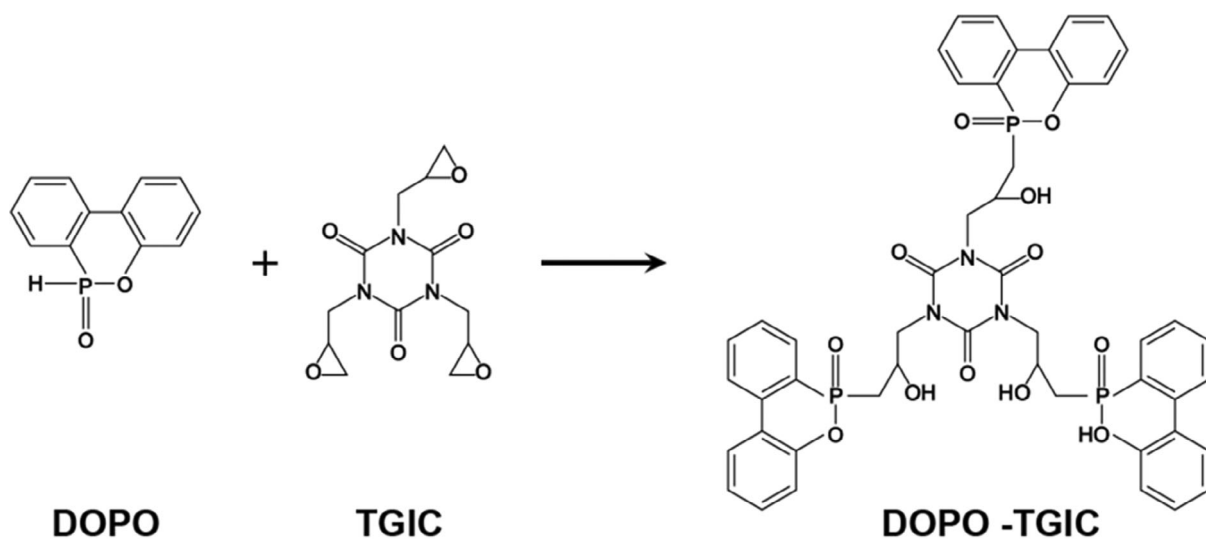
2.3 | Measurements

Fourier transform infrared spectroscopy (FTIR) spectra were obtained using a Nicolet 6700 infrared spectrometer. The powdered samples were thoroughly mixed with KBr and then pressed into pellets.

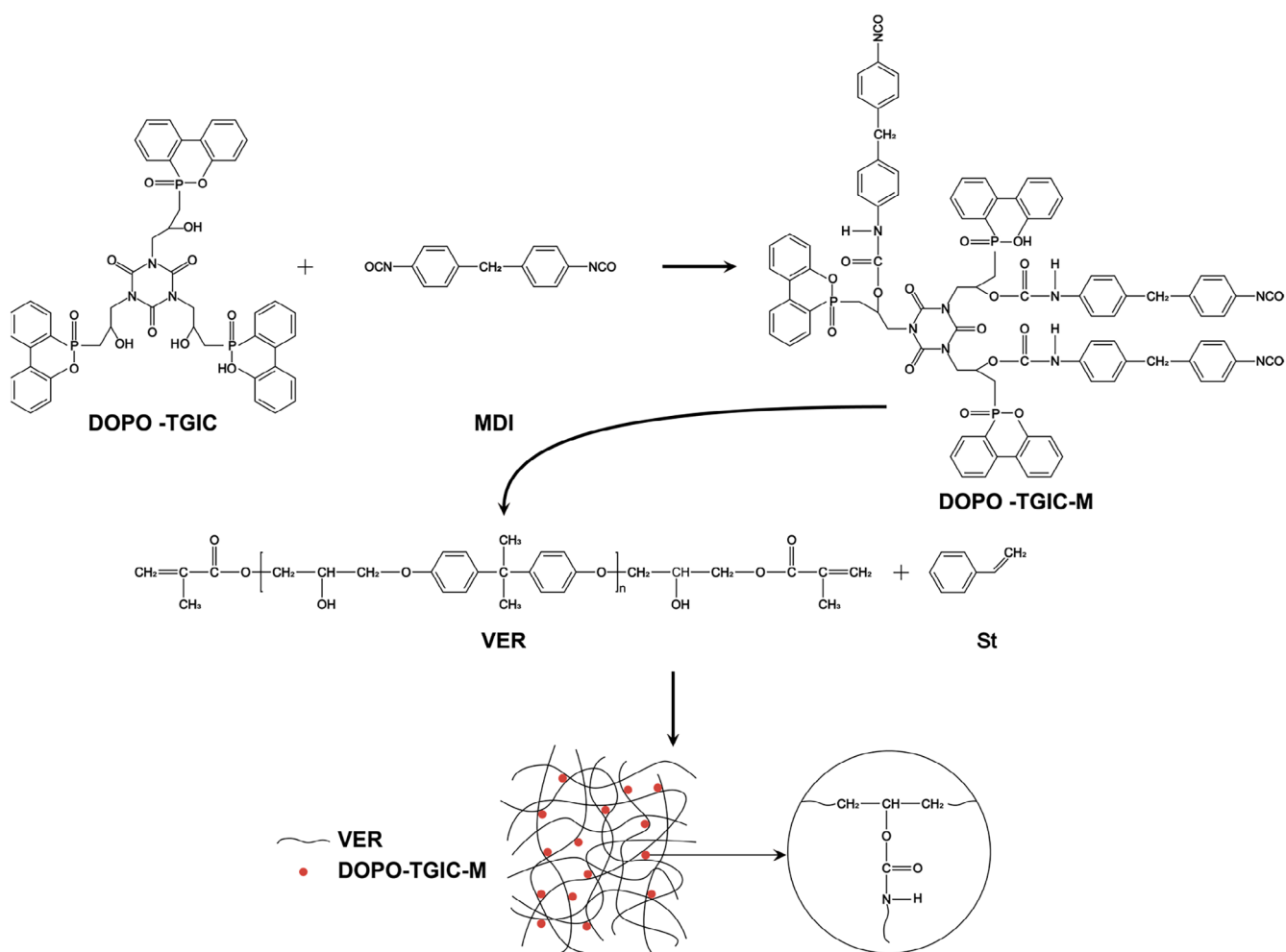
The limited oxygen index (LOI) values were measured on a JF-3 oxygen index meter according to ASTM D2863. The specimen size was 100 mm × 6.5 mm × 3 mm.

Vertical burning (UL-94) tests were performed on a NK8017A vertical burner (Nklsky Instrument Co., Ltd.) based on the UL-94 test standard, and the sample size was 130 mm × 13 mm × 3 mm.

Dynamic mechanical analysis (DMA) was carried out by using a Pyris Diamond dynamic mechanical analyzer (PE company). The samples (size: 60 mm × 10 mm × 2 mm) were tested in a bending mode at a heating rate of 5°C/min and a frequency of 1 Hz in the temperature range of 30–300°C.



SCHEME 1 Synthesis route of DOPO-TGIC.



SCHEME 2 Illustration of cross-linking of flame-retardant VER samples. [Color figure can be viewed at wileyonlinelibrary.com]

TABLE 1 Formulations of VER samples.

Sample	VER (g)	St (g)	MDI (g)	DOPO-TGIC (g)	BPO (g)	P content (wt%)
VER	60	40	–	–	2	–
VER-0.7	60	40	7	8.8	2	0.7
VER-1	60	40	10	12.6	2	1
VER-1.3	60	40	15	18.9	2	1.3

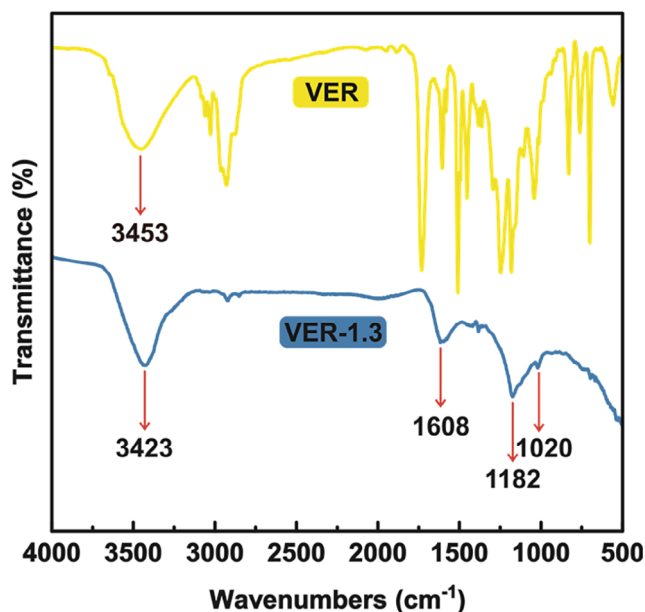


FIGURE 1 FTIR spectra of virgin VER and VER-1.3 samples. [Color figure can be viewed at wileyonlinelibrary.com]

Thermogravimetric analysis (TGA) was conducted on a NETZSCH STA449F3 (TA company) at a heating rate of 10°C/min under nitrogen atmosphere from 40 to 800°C.

Cone calorimetry tests were performed in accordance with the ISO 5660 standard using an FTT0007 cone calorimeter (FTT) under an external flux of 50 kW/m², and the dimensions of all samples were 100 mm × 100 mm × 3 mm.

3 | RESULTS AND DISCUSSION

3.1 | Structural characterization of the flame-retardant VERs

The chemical structures of virgin VER and flame-retardant VER-1.3 samples were characterized by FTIR, with the spectra shown in Figure 1. For virgin VER, the absorption band at 3453 cm⁻¹ was attributed to the stretching vibration of –OH and N–H.²³ In regard to VER-1.3, the peak at 3423 cm⁻¹ could also be observed;

the absorption peak at 1608 cm⁻¹ belonged to the bending vibration of N–H and the stretching vibration of C–N in carbamate structure;²⁴ the peak at 1182 cm⁻¹ was attributed to the stretching vibration of C–O;²⁵ and the peak at 1020 cm⁻¹ was assigned to the stretching vibration of P–O–C,¹⁴ which was a new peak relative to virgin VER. In addition, both absorption peaks of P–H (2437 cm⁻¹) and –NCO (2270 cm⁻¹) disappeared.²⁶ All these FTIR results confirmed that the DOPO-TGIC was covalently linked to the cross-linked network of VER via the bridging action of MDI.

3.2 | Thermal stability of VER

The thermogravimetric (TG) and derivative TG (DTG) curves of VER samples under N₂ atmosphere are presented in Figure 2. The characteristic thermal decomposition parameters, including temperature at 5% weight loss ($T_{5\%}$), temperature at the maximum decomposition rate (T_{max}), the maximum decomposition rate (R_{max}) and char yield at 800°C (CY) are listed in Table 2.

The $T_{5\%}$ and T_{max} of virgin VER were 354 and 418°C, respectively, which were the highest among all samples. The VER-0.7, VER-1 and VER-1.3 samples showed the reduced $T_{5\%}$ and T_{max} values, mainly due to the catalytic decomposition effect of phosphorus-containing group in DOPO-TGIC.^{27–29} Notably, the CY values of the P/N-containing VER samples were much higher than that of virgin VER. For instance, the CY of VER was only 8.8%, while that of VER-1.3% was up to 26.4%, which was increased by twofold. In addition, the P/N-containing VER samples showed decreased R_{max} values relative to virgin VER. Hence, phosphorus- and nitrogen-containing components promoted the carbonization of the VER matrix at high temperatures, thus increasing the CY and reducing the R_{max} .

3.3 | Dynamic mechanical analysis

DMA was used to investigate the effects of DOPO-TGIC and MDI on the glass transition temperature (T_g) and storage modulus (E') of VER, with the curves and data

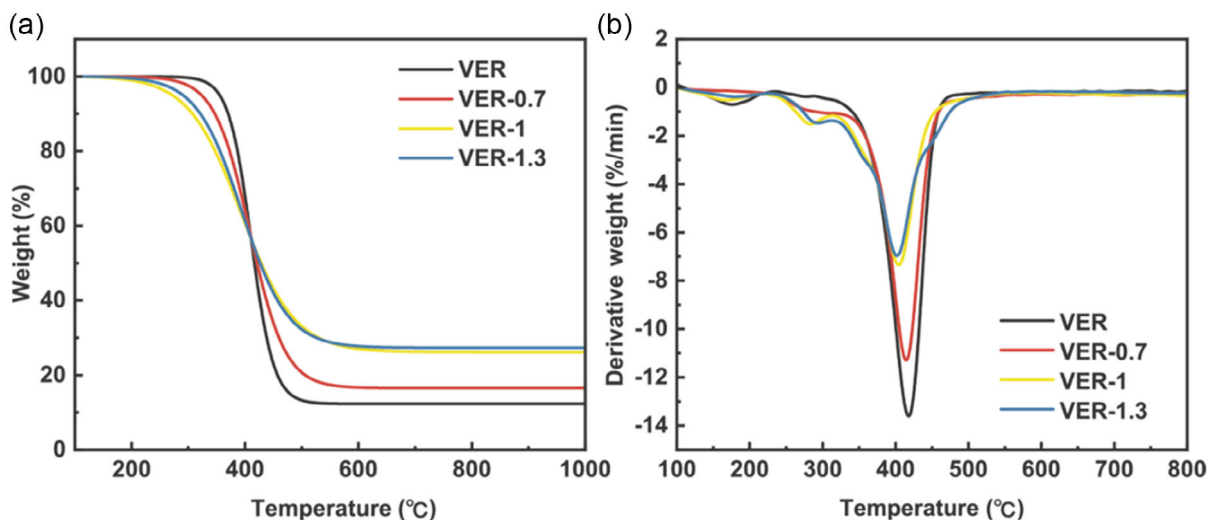


FIGURE 2 (a) TG and (b) DTG curves of VER samples. [Color figure can be viewed at wileyonlinelibrary.com]

TABLE 2 TGA and DMA results of VER samples.

Sample code	$T_{5\%}$ ($^{\circ}\text{C}$)	T_{\max} ($^{\circ}\text{C}$)	R_{\max} (%/min)	CY (%)	T_g ($^{\circ}\text{C}$)	V_e (mol/m^3)	E' at 50°C
VER	354	418	13.6	12.3	115.7	3578	3295
VER-0.7	312	413	11.3	16.4	125.9	3170	2991
VER-1	260	404	7.3	25.7	124.5	1960	2840
VER-1.3	280	402	7.0	26.4	126.9	2599	2986

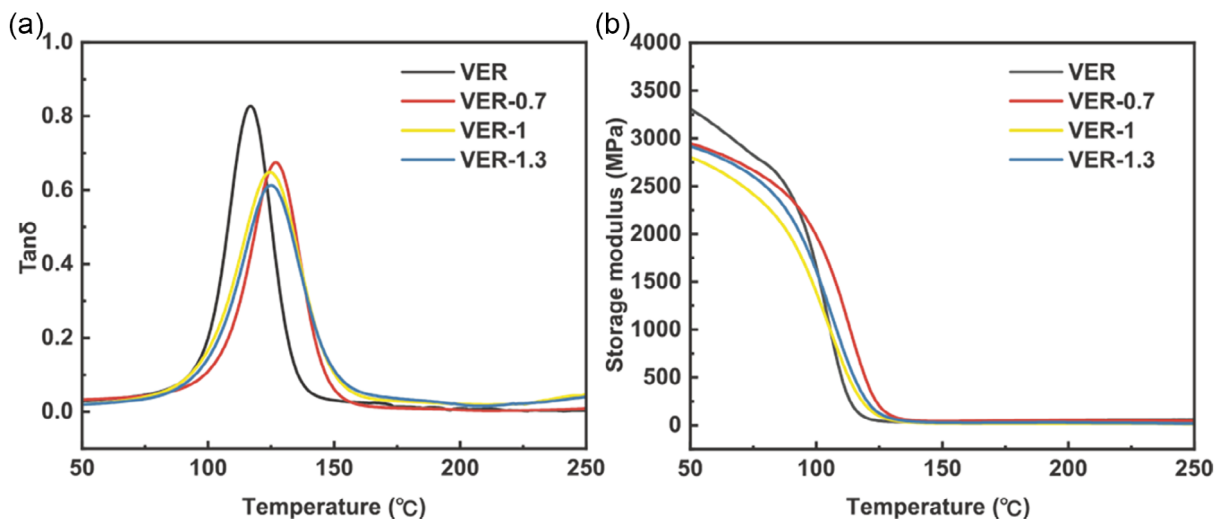


FIGURE 3 (a) $\text{Tan}\delta$ and (b) storage modulus plots of VER samples. [Color figure can be viewed at wileyonlinelibrary.com]

shown in Figure 3 and Table 2. The T_g of VER was 115.7°C . Notably, the T_g values of the flame-retardant VERs (VER-0.7, VER-1 and VER-1.3) were higher than VER, demonstrating the improved heat resistance. Obviously, covalently attaching DOPO-TGIC and MDI to the network of VER contributed to increasing the T_g . Meanwhile, the E' values of VER-0.7, VER-1 and VER-1.3 at

50°C were reduced by about 10% compared with that of VER, indicating that the rigidity of VER was reduced due to the introduction of MDI and DOPO-TGIC. Obviously, using DOPO-TGIC and MDI as additional cross-linking point and bridging agent can increase the cross-linking density (V_e) of VER under the appropriate addition amounts (see Table 2). With the increasing loading levels

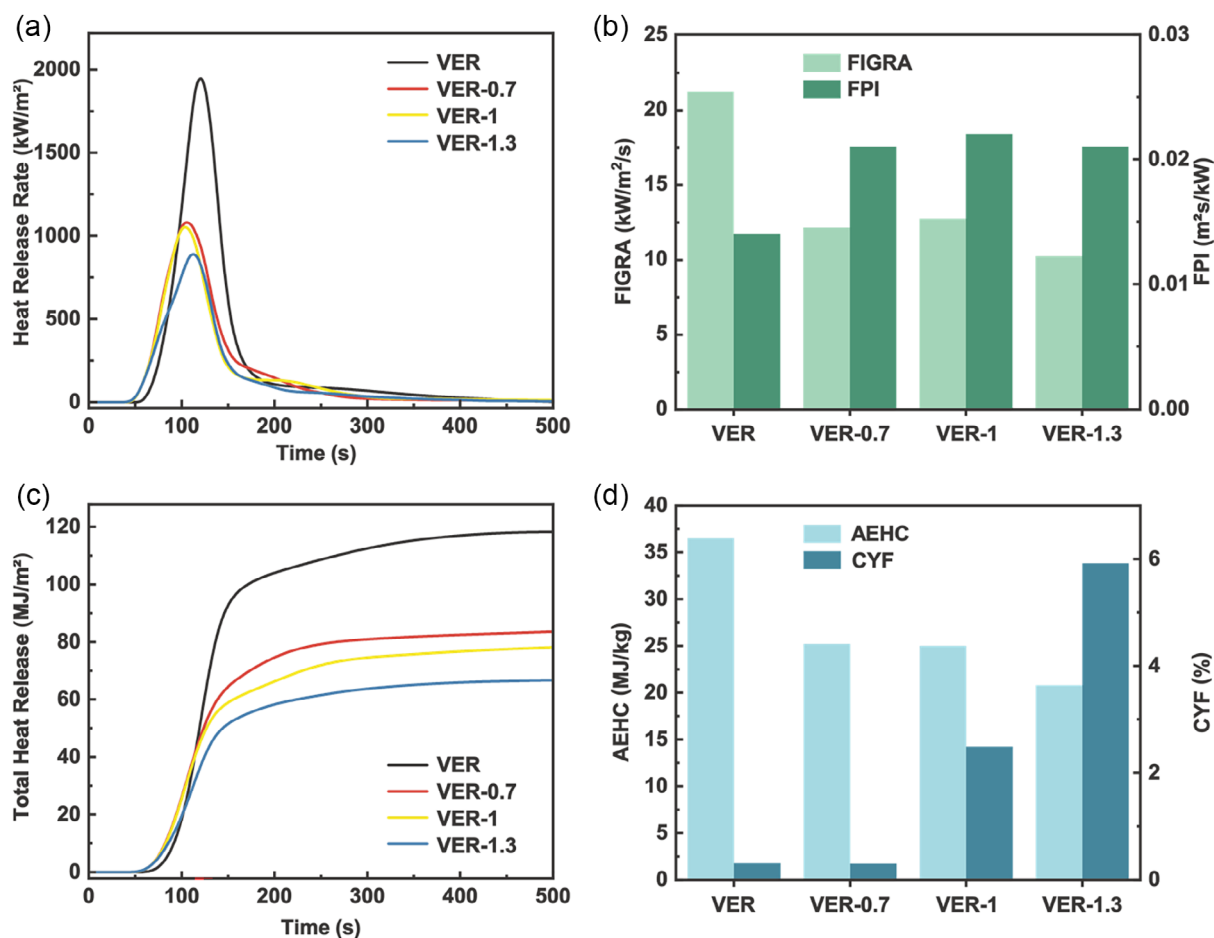


FIGURE 4 (a) HRR curves, (b) FIGRA and FPI values, (c) THR curves, and (d) AEHC and CYF values of VER samples. [Color figure can be viewed at wileyonlinelibrary.com]

of MDI and DOPO-TGIC, the system viscosity gradually increased due to the reaction between MDI and DOPO-TGIC, which hindered the cross-linking reaction of VER, leading to the reduced cross-linking density and rigidity of the thermoset.

3.4 | Flame retardancy and smoke suppression of VER samples

The flame retardancy of VER samples was evaluated by LOI, UL-94 and cone calorimetry tests, with the plots shown in Figure 4. The LOI, UL-94 rating and characteristic combustion parameters, including time to ignition (TTI), peak heat release rate (PHRR), total heat release (THR), fire performance index (FPI), fire growth rate (FIGRA), average effective heat of combustion (AEHC) and char yield at flameout (CYF), are listed in Table 3.

As presented in Table 3, VER suffered from a low LOI of 23%, and cannot achieve any UL-94 rating, demonstrating its poor flame retardancy. With the introduction

of DOPO-TGIC and MDI, the flame retardancy of VER was obviously enhanced. The introduction of DOPO-TGIC and MDI enhanced the self-extinguishing properties of VER samples, making them self-extinguishing after removing the ignitor in the UL-94 tests. Meanwhile, the melt-dripping phenomenon disappeared during the UL-94 tests of the P/N-containing VER samples. Hence, all P/N-containing VER samples achieved the UL-94 V-0 rating. Meanwhile, the LOI values of the P/N-containing VER samples were increased with the increasing phosphorus content, and finally the LOI of VER-1.3 reached 29.5%. Hence, adding DOPO-TGIC and MDI contributed to enhancing the flame retardancy of VER.

The improved flame retardancy of VER can also be confirmed by cone calorimetry data. The PHRR is considered as one of the most important parameters in evaluating the fire safety of the materials.^{30,31} As shown in Figure 4a and Table 3, the neat VER underwent fierce burning and released a large amount of heat upon ignition, and thus its PHRR was the highest among all samples, which reached up to 1972 kW/m². By contrast, the

TABLE 3 The combustion parameters of VER samples.

Sample	LOI (%)	UL-94 rating (3 mm)	TTI (s)	PHRR (kW/m ²)	THR (MJ/m ²)	FPI (m ² s/kW)	FIGRA (kW/m ² /s)	AEHC (MJ/kg)	CYF (%)
VER	23	NR	28	1972 ± 29	118.3 ± 2.2	0.014 ± 0.001	21.2 ± 0.4	36.5 ± 0.5	0.31 ± 0.01
VER-0.7	27.5	V-0	25	1184 ± 11	83.7 ± 1.2	0.021 ± 0.003	12.1 ± 0.6	25.2 ± 0.4	0.31 ± 0.02
VER-1	28.5	V-0	25	1156 ± 12	78.3 ± 1.8	0.022 ± 0.002	12.7 ± 0.5	25.0 ± 0.6	2.49 ± 0.07
VER-1.3	29.5	V-0	19	916 ± 18	66.2 ± 1.6	0.021 ± 0.003	10.2 ± 0.6	20.8 ± 0.4	5.92 ± 0.09

PHRR values of the P/N-containing VER samples were obviously decreased with the introduction of DOPO-TGIC and MDI. When the phosphorus content was 1.3 wt%, the PHRR value of VER-1.3 was 1037 kW/m², with a reduction of 55.6% relative to that of VER, indicating the suppressed heat release. Similar reduction can also be observed in the THR values of the P/N-containing VER samples (see Figure 4c and Table 3). These results confirmed the obvious inhibition of DOPO-TGIC and MDI on the heat release of the matrix during burning. The fire performance index (FPI) and fire growth rate (FIGRA) are two important parameters for assessing the fire safety of the materials. The FPI is the ratio of TTI to PHRR, and the FIGRA is the ratio of PHRR to time to PHRR (T_{PHRR}).^{32,33} As shown in Figure 4b and Table 3, all P/N-containing VER samples showed higher FPI and lower FIGRA values than VER sample. For instance, the FPI of VER-1.3 sample was 0.021 m²s/kW, which was 50% higher than that of virgin VER. The FIGRA of VER-1.3 sample was 10.2 kW/m²/s, which was reduced by 52% relative to that of pure VER. In sum, the P/N-containing VER samples exhibited much greater flame retardancy than VER sample due to the introduction of DOPO-TGIC and MDI.

AEHC, the ratio of the average heat release rate to the average mass loss rate, is used to quantitatively reveal the combustion degree of volatile matters during material combustion.^{34,35} As presented in Figure 4d and Table 3, the AEHC of the P/N-containing VER samples were obviously decreased, compared with that of VER sample. For instance, the AEHC of VER-1.3 was greatly reduced from 36.5 MJ/kg of VER to 20.8 MJ/kg, with a 43.0% reduction. Such result demonstrated the flame-retardant effect of DOPO-TGIC and MDI in the gaseous phase, which suppressed the burning reaction of pyrolysis volatiles and diluted the oxygen concentration.^{36,37}

The CYF values of VER samples are listed in Figure 4d and Table 3. For virgin VER, the CYF was only 0.31%, indicating that it was completely burned out after cone calorimetry test. The CYF of VER-1.3 was increased to 5.92%, with an 18-fold increase relative to that of VER. Hence, the char-forming capacity of the VER matrix was significantly enhanced by the introduction of DOPO-TGIC

and MDI, which was well consistent with the TGA result. The enhancement in carbonization was conducive to maintaining more pyrolysis products in the condensed phase and suppressing the heat release during burning.³⁸ Thus, the obviously improved flame retardancy of the P/N-containing VER samples were mainly due to the reduced burning degree of volatiles and improved char-forming ability.

3.5 | Morphology and composition analyses of char residues

Figure 5 shows the digital and SEM photos of residual chars obtained from cone calorimeter tests. VER was completely burned out, and only left a few broken chars after test (see Figure 5a₁,a₂). On the contrary, VER-1.3 left a dense and intumescent char after burning (see Figure 5b₁,b₂), indicating the condensed-phase flame-retardant effect. As presented in Figure 5c,d, the external surface of VER-1.3 char was continuous and compact, and the internal structure was cancellate. Compared with the VER char, the VER-1.3 char was more effective in suppressing the exchange of heat and oxygen, thus the VER-1.3 sample showed better flame retardancy.³⁹

Figure 6a₁,b₁ display the EDS spectra of residual chars for VER and VER-1.3. The char of VER contained C and O elements, while the P and N elements appeared in the char of VER-1.3. Such result indicated that abundant P/N-containing fragments generated by the pyrolysis of DOPO-TGIC and MDI remained in the condensed phase, which participated in the carbonization of the VER matrix, thus promoting the formation of a compact and intumescent char layer.⁴⁰ The Raman spectra of residual chars are presented in Figure 6a₂,b₂. There were two characteristic peaks appeared in these spectra. One peak located at 1358 cm⁻¹ (D band) corresponded to the disordered carbon, and the other one located at 1588 cm⁻¹ (G band) corresponded to the graphite carbon.⁴¹ The ratio of the integral area of these peaks ($I_{\text{D}}/I_{\text{G}}$) can be used to evaluate the graphitization degree of residual char, and a lower $I_{\text{D}}/I_{\text{G}}$ indicated a higher degree of graphitization.^{42,43} Obviously, the $I_{\text{D}}/I_{\text{G}}$ value of VER-1.3

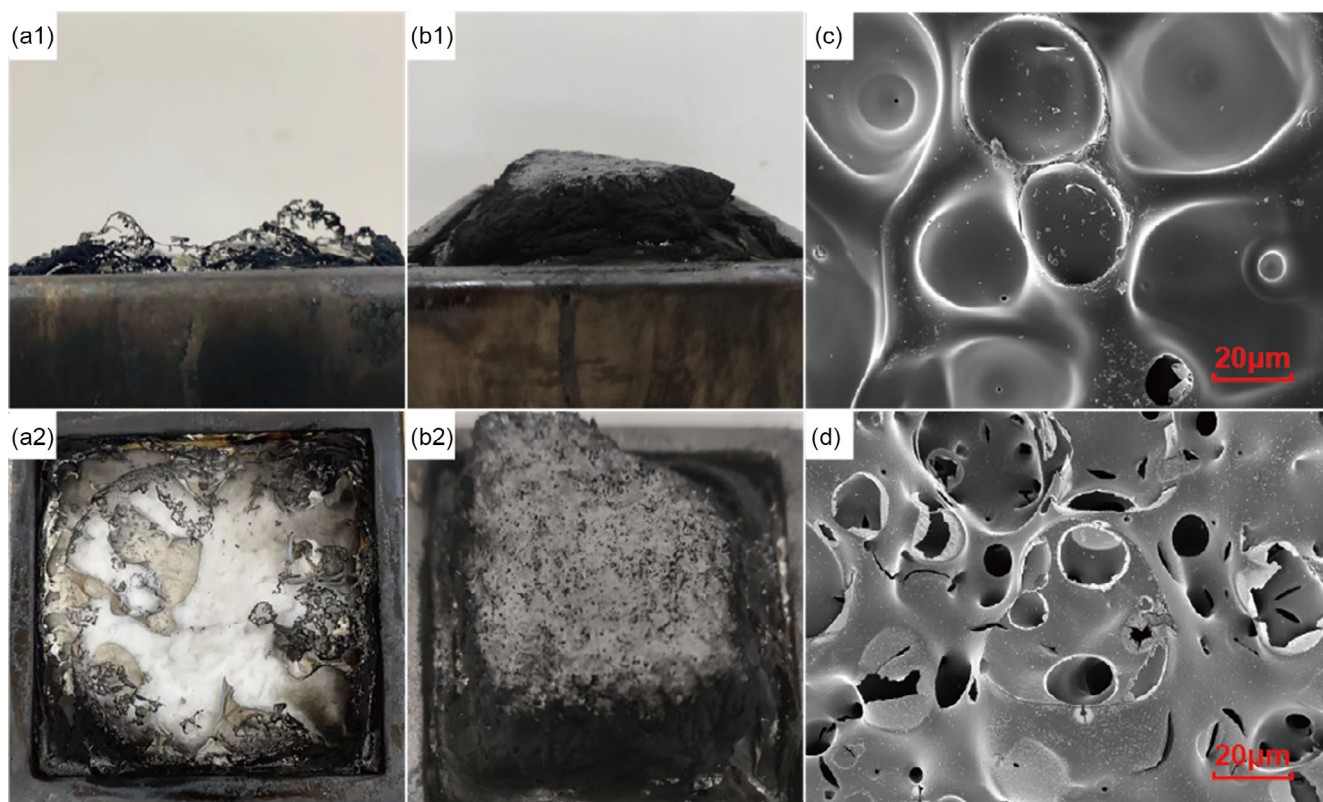


FIGURE 5 Digital photographs of chars for (a₁, a₂) VER and (b₁, b₂) VER-1.3, and SEM images of (c) exterior and (d) interior chars of VER-1.3 after cone calorimeter tests. [Color figure can be viewed at [wileyonlinelibrary.com](#)]

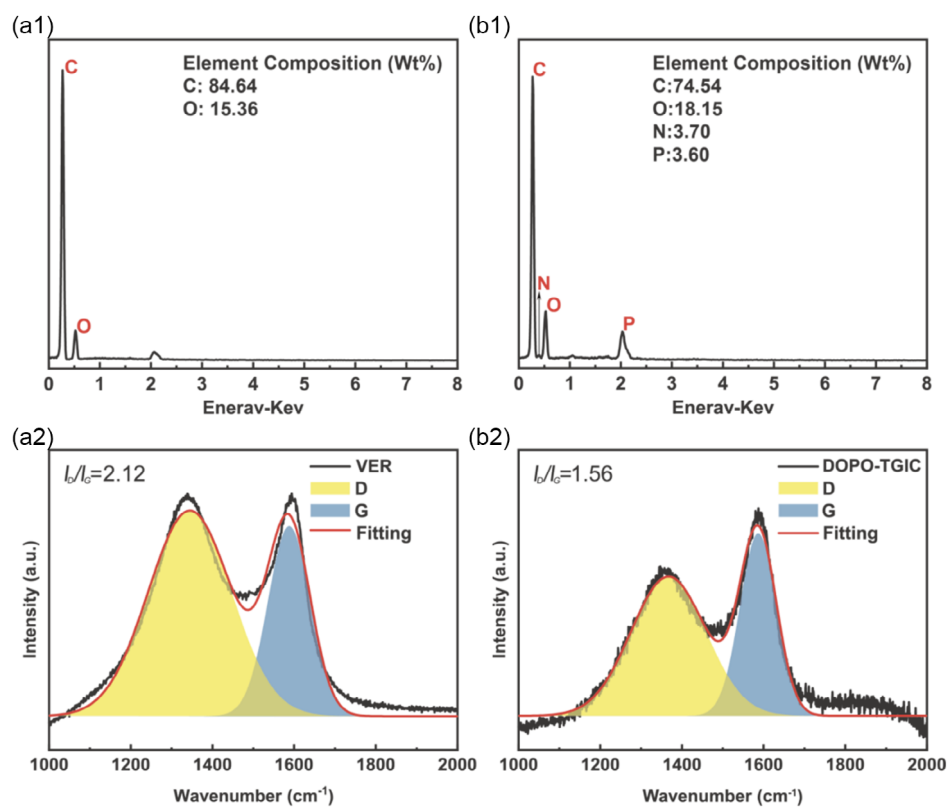


FIGURE 6 The EDS and Raman spectra of chars for VER (a₁, a₂) and VER-1.3 (b₁, b₂) after cone calorimeter tests. [Color figure can be viewed at [wileyonlinelibrary.com](#)]

char was lower than that of VER char, demonstrating the increased degree of graphitization due to the introduction of DOPO-TGIC. The dense and intumescent char with a high degree of graphitization can effectively suppress the heat release of the matrix during burning, thus enhancing the flame retardancy.

4 | CONCLUSIONS

In this study, MDI was applied as a bridge and DOPO-TGIC was used as an additional cross-linking point to address the trade-off between flame retardancy and heat resistance of VER. The DMA and TGA results showed that well-designed VER samples containing DOPO-TGIC and MDI displayed higher T_g and CY values than VER sample, demonstrating the improved heat resistance and carbonization ability. In addition, the P/N-containing VER samples showed better flame retardancy than VER sample due to the incorporation of DOPO-TGIC and MDI, as reflected by much higher LOI values and UL-94 ratings, and obviously lower PHRR and THR values. Therefore, this study offers an effective and facile method to simultaneously enhance the heat resistance and flame retardancy of VER.

AUTHOR CONTRIBUTIONS

Mei Qiu: Data curation (lead); investigation (equal); writing – original draft (equal). **Xi Chen:** Data curation (equal). **Jun Wang:** Project administration (lead); supervision (lead). **Jingsheng Wang:** Data curation (equal). **Kaiwen Chen:** Formal analysis (equal). **Shuang Yang:** Conceptualization (lead). **Siqi Huo:** Writing – review & editing (lead). **Hao Wang:** Supervision (equal).

ACKNOWLEDGMENTS

This work was supported by the Science and Technology Department of Jiangsu Province in China (No. BA2019043), and the Australia Research Council Discovery Early Career Researcher Award (DE230100616).

DATA AVAILABILITY STATEMENT

The data that support the findings of this study are available from the corresponding author upon reasonable request.

ORCID

Shuang Yang  <https://orcid.org/0000-0001-7114-5686>

REFERENCES

- [1] N. Agarwal, A. Singh, I. K. Varma, V. Choudhary, *J. Appl. Polym. Sci.* **1942**, 2008, 108.
- [2] Y. Fang, J. Miao, X. Yang, Y. Zhu, G. Wang, *Chem. Eng. J.* **2020**, 385, 123830.
- [3] J. S. Arrieta, E. Richaud, B. Fayolle, F. Nizeyimana, *Polym. Degrad. Stab.* **2016**, 129, 142.
- [4] A. M. Atta, S. M. El-Saeed, R. K. Farag, *React. Funct. Polym.* **2006**, 66, 1596.
- [5] S. Gaan, G. Sun, K. Hutches, M. H. Engelhard, *Polym. Degrad. Stab.* **2008**, 93, 99.
- [6] Z. Bai, S. Jiang, G. Tang, Y. Hu, L. Song, R. K. K. Yuen, *Polym. Adv. Technol.* **2014**, 25, 223.
- [7] Z. Bai, L. Song, Y. Hu, X. Gong, R. K. K. Yuen, *J. Anal. Appl. Pyrolysis* **2014**, 105, 317.
- [8] Z. Bai, L. Song, Y. Hu, R. K. K. Yuen, *Ind. Eng. Chem. Res.* **2013**, 52, 12855.
- [9] U. Braun, A. I. Balabanovich, B. Schartel, U. Knoll, J. Artner, M. Ciesielski, M. Döring, R. Perez, J. K. W. Sandler, V. Altstädt, T. Hoffmann, D. Pospiech, *Polymer* **2006**, 47, 8495.
- [10] X. Chen, Y. Hu, L. Song, W. Xing, *Polym. Adv. Technol.* **2008**, 19, 393.
- [11] H. Duan, Y. Chen, S. Ji, R. Hu, H. Ma, *Chem. Eng. J.* **2019**, 375, 121916.
- [12] G. Ye, S. Huo, C. Wang, P. Song, Z. Fang, H. Wang, Z. Liu, *Polym. Degrad. Stab.* **2023**, 207, 110235.
- [13] X. Chen, C. Jiao, *Polym. Adv. Technol.* **2010**, 21, 490.
- [14] S. Huo, S. Yang, J. Wang, J. Cheng, Q. Zhang, Y. Hu, G. Ding, Q. Zhang, P. Song, *J. Hazard. Mater.* **2020**, 386, 121984.
- [15] W. Rao, P. Zhao, C. Yu, H.-B. Zhao, Y.-Z. Wang, *Compos. Part B Eng.* **2021**, 211, 108640.
- [16] J. Cheng, H. Duan, S. Yang, J. Wang, Q. Zhang, G. Ding, Y. Hu, S. Huo, *J. Appl. Polym. Sci.* **2020**, 137, 49090.
- [17] J. Ding, W. Shi, *Polym. Degrad. Stab.* **2004**, 84, 159.
- [18] S. Ji, H. Duan, Y. Chen, D. Guo, H. Ma, *Polymer* **2020**, 207, 122917.
- [19] X. Tao, H. Duan, W. Dong, X. Wang, S. Yang, *Polym. Degrad. Stab.* **2018**, 154, 285.
- [20] H. Du, J. Ren, X. Fu, W. Zhang, R. Yang, *Compos. Part B Eng.* **2022**, 238, 109908.
- [21] F.-Q. Zhang, Y.-Z. Zhao, Y.-J. Xu, Y. Liu, P. Zhu, *Compos. Part B Eng.* **2022**, 234, 109697.
- [22] L. Qian, Y. Qiu, N. Sun, M. Xu, G. Xu, F. Xin, Y. Chen, *Polym. Degrad. Stab.* **2014**, 107, 98.
- [23] F. Gao, L. Tong, Z. Fang, *Polym. Degrad. Stab.* **2006**, 91, 1295.
- [24] S. Grishchuk, N. Castellà, A. A. Apostolov, J. Karger-Kocsis, *J. Compos. Mater.* **2011**, 46, 941.
- [25] S. Huo, J. Wang, S. Yang, J. Wang, B. Zhang, B. Zhang, X. Chen, Y. Tang, *Polym. Degrad. Stab.* **2016**, 131, 106.
- [26] S. Jaswal, B. Gaur, *Rev. Chem. Eng.* **2014**, 30, 567.
- [27] C. Wang, S. Huo, G. Ye, P. Song, H. Wang, Z. Liu, *Chem. Eng. J.* **2023**, 451, 138768.
- [28] J. Wang, S. Huo, J. Wang, S. Yang, K. Chen, C. Li, D. Fang, Z. Fang, P. Song, H. Wang, *ACS Appl. Polym. Mater.* **2022**, 4, 3564.
- [29] Q. Chen, L. Liu, A. Zhang, W. Wang, Z. Wang, J. Zhang, J. Feng, S. Huo, X. Zeng, P. Song, *Chem. Eng. J.* **2023**, 454, 140424.
- [30] Y. Lin, B. Yu, X. Jin, L. Song, Y. Hu, *RSC Adv.* **2016**, 6, 49633.
- [31] B. Hu, J. Wang, J. Wang, S. Yang, C. Li, F. Wang, S. Huo, P. Song, Z. Fang, H. Wang, *Polym. Degrad. Stab.* **2022**, 204, 110092.
- [32] H. Ma, L. Tong, Z. Xu, Z. Fang, Y. Jin, F. Lu, *Polym. Degrad. Stab.* **2007**, 92, 720.

- [33] Q. Shi, S. Huo, C. Wang, G. Ye, L. Yu, Z. Fang, H. Wang, Z. Liu, *Polym. Degrad. Stab.* **2022**, 203, 110065.
- [34] S. Huo, T. Sai, S. Ran, Z. Guo, Z. Fang, P. Song, H. Wang, *Compos. Part B Eng.* **2022**, 234, 109701.
- [35] Z. Zhao, J. Wang, J. Wang, K. Chen, B. Zhang, Q. Chen, P. Guo, X. Wang, F. Liu, S. Huo, *React. Funct. Polym.* **2022**, 170, 105103.
- [36] B. Perret, B. Schartel, K. Stöß, M. Ciesielski, J. Diederichs, M. Döring, J. Krämer, V. Altstädt, *Macromol. Mater. Eng.* **2011**, 296, 14.
- [37] B. Perret, B. Schartel, K. Stöß, M. Ciesielski, J. Diederichs, M. Döring, J. Krämer, V. Altstädt, *Eur. Polym. J.* **2011**, 47, 1081.
- [38] L. Qian, L. Ye, Y. Qiu, S. Qu, *Polymer* **2011**, 52, 5486.
- [39] X. Qian, L. Song, S. Jiang, G. Tang, W. Xing, B. Wang, Y. Hu, R. K. K. Yuen, *Ind. Eng. Chem. Res.* **2013**, 52, 7307.
- [40] E. J. Robinette, S. Ziaee, G. R. Palmese, *Polymer* **2004**, 45, 6143.
- [41] F. Wu, J. Wang, J. Wang, K. Chen, S. Yang, S. Huo, H. Wang, *J. Polym. Sci.* **2023**, 61, 422.
- [42] K. A. Salmeia, S. Gaan, *Polym. Degrad. Stab.* **2015**, 113, 119.
- [43] G. Ye, S. Huo, C. Wang, Q. Shi, L. Yu, Z. Liu, Z. Fang, H. Wang, *Compos. Part B Eng.* **2021**, 227, 109395.

How to cite this article: M. Qiu, X. Chen, J. Wang, J. Wang, K. Chen, S. Yang, S. Huo, H. Wang, *J. Appl. Polym. Sci.* **2023**, 140(23), e53937.
<https://doi.org/10.1002/app.53937>